

HESS upper limits for Kepler's supernova remnant

F. Aharonian^{1,13}, A. G. Akhperjanian², U. Barres de Almeida^{8,*}, A. R. Bazer-Bachi³, B. Behera¹⁴, M. Beilicke⁴, W. Benbow¹, D. Berge^{1,**}, K. Bernlöhr^{1,5}, C. Boisson⁶, O. Bolz¹, V. Borrel³, I. Braun¹, E. Brion⁷, J. Brucker¹⁶, R. Bühler¹, T. Bulik²⁴, I. Büsching⁹, T. Boutelier¹⁷, S. Carrigan¹, P. M. Chadwick⁸, L.-M. Chounet¹⁰, A. C. Clapson¹, G. Coignet¹¹, R. Cornils⁴, L. Costamante^{1,28}, M. Dalton⁵, B. Degrange¹⁰, H. J. Dickinson⁸, A. Djannati-Atai¹², W. Domainko¹, L. O'C. Drury¹³, F. Dubois¹¹, G. Dubus¹⁷, J. Dyks²⁴, K. Egberts¹, D. Emmanoulopoulos¹⁴, P. Espigat¹², C. Farnier¹⁵, F. Feinstein¹⁵, A. Fiasson¹⁵, A. Förster¹, G. Fontaine¹⁰, M. Füßling⁵, Y. A. Gallant¹⁵, B. Giebels¹⁰, J. F. Glicenstein⁷, B. Glück¹⁶, P. Goret⁷, C. Hadjichristidis⁸, D. Hauser¹, M. Hauser¹⁴, G. Heinzelmann⁴, G. Henri¹⁷, G. Hermann¹, J. A. Hinton²⁵, A. Hoffmann¹⁸, W. Hofmann¹, M. Holleran⁹, S. Hoppe¹, D. Horns⁴, A. Jacholkowska¹⁵, O. C. de Jager⁹, I. Jung¹⁶, K. Katarzyński²⁷, E. Kendziorra¹⁸, M. Kerschhaggl⁵, B. Khélifi¹⁰, D. Keogh⁸, Nu. Komin¹⁵, K. Kosack¹, G. Lamanna¹¹, I. J. Latham⁸, M. Lemoine-Goumard^{10,***}, J.-P. Lenain⁶, T. Lohse⁵, J. M. Martin⁶, O. Martineau-Huynh¹⁹, A. Marcowith¹⁵, C. Masterson¹³, D. Maurin¹⁹, T. J. L. McComb⁸, R. Moderski²⁴, E. Moulin⁷, M. Naumann-Godo¹⁰, M. de Naurois¹⁹, D. Nedbal²⁰, D. Nekrassov¹, S. J. Nolan⁸, S. Ohm¹, J.-P. Olive³, E. de Oña Wilhelmi¹², K. J. Orford⁸, J. L. Osborne⁸, M. Ostrowski²³, M. Panter¹, G. Pedalletti¹⁴, G. Pelletier¹⁷, P.-O. Petrucci¹⁷, S. Pita¹², G. Pühlhofer¹⁴, M. Punch¹², A. Quirrenbach¹⁴, B. C. Raubenheimer⁹, M. Raue¹, S. M. Rayner⁸, M. Renaud¹, J. Ripken⁴, L. Rob²⁰, S. Rosier-Lees¹¹, G. Rowell²⁶, B. Rudak²⁴, J. Ruppel²¹, V. Sahakian², A. Santangelo¹⁸, R. Schlickeiser²¹, F. M. Schöck¹⁶, R. Schröder²¹, U. Schwanke⁵, S. Schwarzburg¹⁸, S. Schwemmer¹⁴, A. Shalchi²¹, H. Sol⁶, D. Spangler⁸, Ł. Stawarz²³, R. Steenkamp²², C. Stegmann¹⁶, G. Superina¹⁰, P. H. Tam¹⁴, J.-P. Tavernet¹⁹, R. Terrier¹², C. van Eldik¹, G. Vasileiadis¹⁵, C. Venter⁹, J. P. Vialle¹¹, P. Vincent¹⁹, M. Vivier⁷, H. J. Völk¹, F. Volpe^{10,28}, S. J. Wagner¹⁴, M. Ward⁸, A. A. Zdziarski²⁴, and A. Zech⁶

(Affiliations can be found after the references)

Received 15 January 2008 / Accepted 12 June 2008

ABSTRACT

Aims. Observations of Kepler's supernova remnant (G4.5+6.8) with the HESS telescope array in 2004 and 2005 with a total live time of 13 h are presented.

Methods. Stereoscopic imaging of Cherenkov radiation from extensive air showers is used to reconstruct the energy and direction of the incident gamma rays.

Results. No evidence for a very high energy (VHE: >100 GeV) gamma-ray signal from the direction of the remnant is found. An upper limit (99% confidence level) on the energy flux in the range 230 GeV–12.8 TeV of 8.6×10^{-13} erg cm⁻² s⁻¹ is obtained.

Conclusions. In the context of an existing theoretical model for the remnant, the lack of a detectable gamma-ray flux implies a distance of at least 6.4 kpc. A corresponding upper limit for the density of the ambient matter of 0.7 cm⁻³ is derived. With this distance limit, and assuming a spectral index $\Gamma = 2$, the total energy in accelerated protons is limited to $E_p < 8.6 \times 10^{49}$ erg. In the synchrotron/inverse Compton framework, extrapolating the power law measured by RXTE between 10 and 20 keV down in energy, the predicted gamma-ray flux from inverse Compton scattering is below the measured upper limit for magnetic field values greater than 52 μ G.

Key words. gamma rays: observations – ISM: supernova remnants – ISM: individual objects: Kepler's SNR, SN1604, G4.5+6.8

1. Introduction

It is widely believed that the bulk of the Galactic cosmic rays (CR) with energies up to at least several 100 TeV originates from supernova explosions (see for example Drury et al. 1994). This implies copious amounts of very high energy (VHE: >100 GeV) nuclei and electrons in the shells of supernova remnants (SNRs). These particles can produce VHE gamma rays in interactions of nucleonic cosmic rays with ambient matter, via inverse Compton (IC) scattering of VHE electrons off ambient photons,

as well as from electron Bremsstrahlung on ambient matter. Therefore SNRs are promising targets for observations of VHE gamma rays.

In October 1604 several astronomers, among them Johannes Kepler, observed a “new star” which today is believed to have been a bright supernova (SN) at the Galactic coordinates $l = 4.5^\circ$ and $b = 6.8^\circ$. The remnant of this supernova has since been a target of observations covering the entire electromagnetic spectrum. In the radio regime, Dickel et al. (1988) determined a mean angular size of $\sim 200''$ and a mean expansion law $R \propto t^{0.50}$, where R is the radius and t is the time. However, the expansion parameter $x = \dot{R}t/R$ varies considerably around the SNR shell, $0.35 < x < 0.65$, possibly indicating spatial inhomogeneities in the circumstellar gas density. In a very recent

* Supported by CAPES Foundation, Ministry of Education of Brazil.

** Now at CERN, Geneva, Switzerland.

*** Now at CENBG, Gradignan, France.

paper by Vink (2008) these properties, and the general asymmetry of the remnant, have been basically confirmed through X-ray measurements. They also allowed the analysis of a high-velocity synchrotron filament in the eastern part of the remnant with $x = 0.7$.

In addition, the distance d to the SNR is still under debate. Reynoso & Goss (1999) report on an HI absorption feature in VLA data and use the Galactic rotation model of Fich et al. (1989) to calculate a lower limit $d > (4.8 \pm 1.4)$ kpc. They also give an upper limit on the distance due to the lack of absorption by an HI cloud at 6.4 kpc. The authors remark that these values involve uncertainties because of the proximity of Kepler’s SNR to the Galactic center. In contrast, Sankrit et al. (2005) and subsequently Blair et al. (2007) have given a lower source distance of $d = 3.9(+1.9 - 0.9)$ kpc, from an absolute shock velocity $\sim 1660 \pm 120$ km s⁻¹ derived from the H α emission line width of a Balmer-dominated filament that is located in the northwestern region. The line broadening, taken as an indication of the downstream thermal gas temperature, was used to determine the shock velocity. We shall return to this question in the discussion section.

Finally, the type of the supernova is not undisputed. From the reconstructed light curve Baade (1943) claimed that it was a type Ia SN, but Doggett & Branch (1985) argued that the light curve is also consistent with a type II-L. Smith et al. (1989) and Kinugasa & Tsunemi (1999) observed a relative overabundance of heavy elements that agrees with type Ia nucleosynthesis models, while Decourchelle & Ballet (1994) saw more evidence that Kepler’s SNR is the remnant of a core-collapse SN. Its position, 500–750 pc above the Galactic plane, is more consistent with a type Ia than a type II SN, as a SN of the latter type is expected to be confined to the region of high gas density found in the plane. However, in the case of a core-collapse event this might be explained through the model of a runaway star, as proposed by Bandiera (1987). More recently, theoretical modeling of the detailed thermal line spectra obtained with XMM (Cassam-Chenaï et al. 2004) led Badenes et al. (2005) to the conclusion that the X-ray spectrum is best fit by a type Ia SN, a view also expressed by Blair (2005). Most recently Reynolds et al. (2007) reported on deep Chandra observations and argued from the high abundance of iron and the very low abundance of oxygen that the progenitor of Kepler’s SNR has been a type Ia SN. Therefore it appears that the observational evidence is finally converging on a type Ia event.

In this paper observations of Kepler’s SNR with the HESS telescope array are described. An upper limit on the integrated energy flux above 230 GeV is derived. Combining this HESS result with the theoretical predictions of Berezhko et al. (2006) suggests a lower limit on the distance, close to the upper limit given by Reynoso & Goss (1999), if Kepler’s SN is a priori assumed to be of type Ia.

2. HESS data and analysis

HESS is an array of four imaging atmospheric Cherenkov telescopes situated in the Khomas Highland of Namibia (Hinton 2004). Kepler’s SNR was observed with the entire telescope array between May 2004 and July 2005 for a total observation time of 14 h. The observations were made in *wobble mode*, where the tracking position is offset from the source center (RA 17^h30^m42.12^s, Dec -21°28′59.9″ J2000.0). Offsets ranging from 0.40° to 0.85° were used. The data were taken at zenith angles between 1° and 49°, with a mean zenith angle

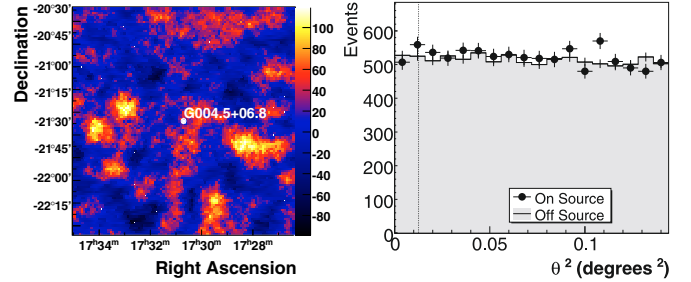


Fig. 1. *Left:* sky map of excess events around the position of Kepler’s SNR with oversampling radius 0.112°; *right:* distribution of the squared angular distance of gamma-ray-like events to the center of the remnant (ON) and the center of three control regions (OFF) with the same distance to the pointing position as the ON region. The vertical dotted line denotes the standard selection cut for point sources used by HESS.

of 13°. After applying the standard HESS data-quality criteria a total of ~ 13 h live time were available for the analysis. The analysis is performed using the standard analysis techniques (Aharonian et al. 2004, 2005).

An event is counted as an ON-source event if its direction is reconstructed within 0.112° from the direction of the source, given that Kepler’s SNR is expected to be point-like for HESS¹. This is a reasonable assumption as the angular size of the remnant in radio and X-rays wavelengths is 200″ (=0.06°).

As the data were taken in wobble mode, the background estimation can be done using OFF-source regions in the same field of view with the same size and offset angle (angular distance to the pointing position) as the source region (Berge et al. 2007).

A second independent analysis, used to cross-check the results, is based on the three-dimensional modeling of the Cherenkov light in the shower (Lemoine-Goumard et al. 2006). The background estimation for this second analysis was done similarly.

With the standard analysis 827 ON and 8855 OFF events (with a normalization of $\alpha = 0.0911$) are measured, resulting in an excess of 20 ± 30 events. The total significance of the excess from the direction of Kepler’s SNR (calculated using Eq. (17) of Li & Ma 1983) is 0.68 standard deviations. Figure 1 shows in the left panel a sky map of excess events around the position of Kepler’s SNR and in the right panel the distribution of the squared angular distance of observed gamma-ray candidates from the center of the remnant in comparison to OFF data. The angular distribution of the ON events is compatible with the distribution of the OFF events. There is no evidence for a gamma-ray signal from Kepler’s SNR.

The approach of Feldman & Cousins (1998) is used to calculate the upper limits on the integrated photon flux above 230 GeV. At a confidence level of 99% an upper limit of $F(>230 \text{ GeV}) < 9.3 \times 10^{-13} \text{ cm}^{-2} \text{ s}^{-1}$ for an assumed photon index of $\Gamma = 2.0$ is derived. At the same confidence level an upper limit on the energy flux of $F_E(230 \text{ GeV} - 12.8 \text{ TeV}) < 8.6 \times 10^{-13} \text{ erg cm}^{-2} \text{ s}^{-1}$ in the HESS energy range for this data set (230 GeV – 12.8 TeV) is derived. The assumed index of 2 requires an upper bound for the integration range to avoid a divergent energy flux.

These values depend only weakly on the assumed photon index for reasonable values (i.e. $2.0 < \Gamma < 3.0$).

¹ The value 0.112° comes from a cut on the squared angular distance of 0.0125 deg² used in the standard HESS analysis.

3. Discussion

To put the observed upper limit on the gamma-ray emission into perspective, the above result is compared with theoretical expectations. Such expectations have recently been formulated by Berezhko et al. (2006) (BKV), using a non-linear kinetic theory of cosmic-ray acceleration in SNRs. This model is based on a time-dependent, spherically symmetric solution of the CR transport equation, coupled to the dynamics of the thermal gas. The key assumption is that the explosion was a standard type Ia event in a circumstellar medium at rest, representing an explosion energy $E_{\text{SN}} \approx 10^{51}$ erg and an ejected mass of $1.4 M_{\odot}$. For a given distance the hydrogen density can then be derived from the known angular expansion velocity and size of the remnant, assumed to be given by the radio data of Dickel et al. (1988) and averaging these data over the azimuthal non-uniformities of the projected SNR shell. The use of such an average value for the angular velocity of the shock and the implied assumption of a uniform circumstellar density is a necessary approximation within such a one-dimensional model which is meant to describe the overall physics of a point explosion. On the other hand, the systematic errors which these assumptions introduce are difficult to estimate, especially in the transition between sweep-up and adiabatic phase. BKV obtained the spectrum and the spatial distribution of CR in the remnant and the density of thermal gas. On this basis they then calculated the expected flux of non-thermal emission (Fig. 2). To account for the uncertainties in the distance estimate this was done for a distance range from 3.4–7 kpc. The derived ambient density varies with the distance assumed and the numerical results show that for a distance d as low as 4.8 kpc the SNR has reached the Sedov phase. Therefore the predicted integral hadronic gamma-ray flux roughly decreases with distance $\propto E_{\text{SN}}^2/d^7$, in agreement with the calculations shown in Fig. 2. Approximating the emission measure for free-free emission by $\text{EM} \sim N_{\text{H}} M_{\text{sw}}$, where M_{sw} denotes the swept-up circumstellar mass, EM scales in the same way with E_{SN} and d as does the gamma-ray flux.

To compare the given upper limit with the model prediction, the quantity $\tilde{F}(> E) = E \cdot F(> E)$ is determined. Here $F(> E)$ is the upper limit on the integrated Flux above the energy E . For $E = 230$ GeV the value for \tilde{F} is $\tilde{F}(> 230 \text{ GeV}) = 3.4 \times 10^{-13} \text{ erg cm}^{-2} \text{ s}^{-1}$. The resulting integrated upper limits are plotted in Fig. 2 for several energies in the range $0.23 < (E/1 \text{ TeV}) < 3.7$. Note that for these values no upper bound for the integration is needed as the quantity $F(> E)$ decreases with energy for spectral indices greater than $\Gamma = 1.0$.

Within the context of the model of BKV, the HESS upper limits rule out distances smaller than 6.4 kpc for $E_{\text{SN}} \geq 10^{51}$ erg and thus densities larger than 0.7 cm^{-3} , and values of EM in excess of $\geq 13 M_{\odot} \text{ cm}^{-3}$. The mean shock velocity is then $\approx 4000 \text{ km s}^{-1}$, and the SNR is just in transition from the sweep-up phase to the Sedov phase.

From SN explosion theory (see BKV, and references therein) a lower limit of $E_{\text{SN}} \sim 0.8 \times 10^{51}$ erg appears appropriate for type Ia SNe. Considering such a reduced explosion energy, the expected flux in gamma rays would be lower and therefore the HESS upper limit would result in a reduced lower limit on the distance of $d > 6.0$ kpc.

While in the BKV model the above value of EM that corresponds to the upper limit of HESS agrees quite well with the overall number recently derived by Blair et al. (2007) from their measurements, the distances of 6.4 and 6.0 kpc differ significantly from the value adopted by these authors, whose distance estimate is within the errors smaller than 5.8 kpc (see Sect. 1).

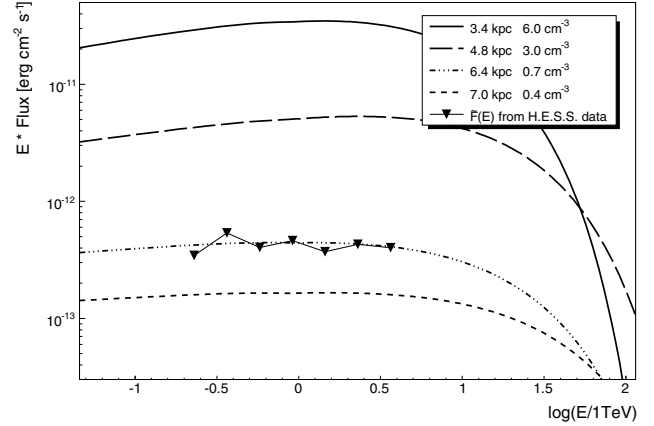


Fig. 2. Comparison of the upper limits on $\tilde{F}(E)$ with predictions of BKV.

On the other hand, Blair et al. (2007) derived their distance value from an optical filament in the northwestern region which has the smallest expansion parameter found in the radio and X-ray observations all around the remnant. It is also interesting to note that the determination of the shock velocity from the $\text{H}\alpha$ line broadening should involve a CR-modified shock, in contrast to the assumption of Sankrit et al. (2005). Efficient particle acceleration in the SNR modifies the shock, whereby part of the gas compression – but only a very small part of the gas heating – occurs in a smooth precursor, in which the CR pressure gradient slows down the incoming gas flow. This is followed by the so-called subshock (Drury & Völk 1981) where most of the gas heating occurs (Berezhko & Ellison 1999). The compression ratio σ_s of the subshock is smaller than the overall shock compression ratio σ . Such a shock structure implies that the shock velocity corresponding to the downstream thermal motions is the subshock velocity $V_s^{\text{sub}} = \sigma_s/\sigma \times V_s$, where V_s is the total shock velocity. In other words, a higher overall shock velocity is required to achieve the same gas heating if in addition CR are accelerated. Therefore the source distance derived from the width of the $\text{H}\alpha$ line is $\sigma_s/\sigma < 1$ times the true source distance if derived without particle acceleration. This may imply a substantial systematic error. In the BKV model for Kepler, in spherical symmetry it is $\sigma_s/\sigma \approx 0.4$ for an assumed distance of 4.8 kpc, and still equal to 0.6 for $d = 6.4$ kpc. Therefore the nominal distance $d = 4$ kpc adopted by Blair et al. (2007) is equivalent to $d = 6.6$ kpc, if the northwestern region considered is indeed one where acceleration is efficient. If particle acceleration is not efficient in this region, then the correction factor is unity. Even a slight modification $\sigma_s/\sigma \approx 0.9$ of the shock makes the source distances compatible.

Independent of particle acceleration models one can use the HESS upper limit also to constrain the content of energetic particles in the remnant. Using the limit on the flux in the range between 0.23 TeV and 12.8 TeV, an upper limit on the gamma-ray luminosity $L_{\gamma, \text{max}} = 4\pi F_E d^2$ can be estimated, where F_E is the integrated energy flux upper limit. In this range then $L_{\gamma, \text{max}} < 1.0 \times 10^{32} \cdot (d/\text{kpc})^2 \text{ erg s}^{-1}$ is derived. For power-law spectra, the δ -function approximation

$$\phi_{\pi}(E_{\pi}) \approx \frac{cn}{K_{\pi}} \sigma_{\text{pp}} \left(\frac{E_{\pi}}{K_{\pi}} \right) n_{\text{p}} \left(\frac{E_{\pi}}{K_{\pi}} \right) \quad (1)$$

can be used to relate the spectra of pions (or gamma rays) to those of the primary protons (Aharonian & Atoyan 2000); here ϕ_{π} is the pion (or gamma-ray) production rate, n the gas

density, n_p the number of protons and K_π is the mean fraction of the kinetic energy of the proton transferred to the secondary π^0 -meson per collision. The rest mass of the proton is neglected. For spectral indices $\Gamma = 2-3$, $K_\pi = 0.17$ can be used to approximate the pion spectrum (Aharonian & Atoyan 2000), a similar value also applies for gamma-ray spectra. At high energy, the proton-proton cross-section σ_{pp} is only weakly energy dependent and can be approximated with $\sigma_{pp} \simeq 40$ mb (Gaisser 1990). The HESS data probe proton energies in the range from about 1 to 100 TeV; using Eq. (1) and assuming an index $\Gamma = 2.0$, a limit on the energy in protons of $E_p < 4.9 \times 10^{47} (d/\text{kpc})^2 (n/\text{cm}^{-3})^{-1}$ erg can be derived. Extrapolating to the 1 GeV to 1 PeV range results in an upper limit on the total energy in accelerated protons of $1.5 \times 10^{48} \text{ erg } (d/\text{kpc})^2 (n/\text{cm}^{-3})^{-1}$. Using $d = 6.4$ kpc and $n = 0.7 \text{ cm}^{-3}$ (dashed-3-dotted line in Fig. 2) this results in $E_p < 8.6 \times 10^{49}$ erg, i.e. $\sim 9\%$ of the assumed energy $E_{\text{SN}} = 10^{51}$ erg. This is of the order of what is expected for an average cosmic-ray source in the form of a SNR. Assuming $E_{\text{SN}} = 10^{51}$ erg and using the argument of BKV that $d < 7$ kpc, in agreement with the observational argument of Reynoso & Goss (1999), the expected gamma-ray flux should not be lower than the HESS upper limit by more than a factor 2 as can be seen in Fig. 2.

In another scenario the gamma-ray emission can be produced via IC scattering by VHE electrons off ambient photons mainly from the cosmic microwave background (CMB). The same electrons emit synchrotron X-ray radiation by being deflected by magnetic fields in the SNR. The energy of the gamma-ray photons is coupled to that of the X-ray photons according to $(E_X/1 \text{ keV}) \sim 0.07 \cdot (E_\gamma/1 \text{ TeV}) (B/10 \mu\text{G})$ in the case of the CMB as target photon field for the IC scattering. If the observed hard X-ray radiation (Allen et al. 1999), with a flux normalisation of $6.2 \times 10^{-5} \text{ cm}^{-2} \text{ s}^{-1} \text{ keV}^{-1}$ and a slope of -3.0 ± 0.2 , is synchrotron radiation (with the corresponding energy flux² f_X) the energy flux in gamma rays is given by $f_\gamma(E_\gamma)/f_X(E_X) \sim \xi 0.1 (B/10 \mu\text{G})^{-2}$ (Aharonian et al. 1997). The factor ξ takes into account possible differences in the source sizes in X-ray and gamma-ray wavelengths. We assume here $\xi \sim 1$.

In principle one could try to use the above relations to obtain a lower limit on the magnetic field strength since the upper limit on the flux in particular constrains any IC component. For this purpose the energy flux from X-ray synchrotron emission at an energy corresponding to a given energy probed in VHE gamma rays has to be known either from measurements or from detailed modeling. The interval in E_X that corresponds to the observed gamma-ray energy interval $0.23 < E_\gamma/1 \text{ TeV} < 3.7$ is $\sim (B/10 \mu\text{G}) \times (0.02-0.26) \text{ keV}$, whereas the energy interval in which the total non-thermal X-ray flux is known is 10–20 keV (Allen et al. 1999). The X-ray instrument PCA on board *RXTE*, with which the underlying data were obtained, has no imaging capabilities and therefore the measured spectrum is the overall spectrum of the field of view of the instrument (which is 1°). Although it is expected that the measured photon flux is indeed from Kepler's SNR because of its position well above the plane, the X-ray flux has to be treated as an upper limit. Unfortunately there is no published analysis of the non-thermal flux from *Chandra* data covering the entire remnant. It is also not possible to unambiguously disentangle the non-thermal and the thermal

contribution to the total spectrum measured by *XMM-Newton* (Cassam-Chenaï, private communication).

In the energy range around a few keV the extrapolation of the observed hard X-ray flux to lower energies involves considerable uncertainties. Nevertheless, in almost all scenarios the extrapolation of the power-law spectrum measured between 10 and 20 keV (with a spectral index of $\Gamma = 3.0$) should be an upper limit to the X-ray to UV flux. With this extrapolation an upper limit on the gamma-ray flux from IC scattering for a given magnetic field can be calculated using the above formulas.

For magnetic field values greater than $52 \mu\text{G}$ the resulting predicted upper limit on the IC flux would be less than the measured upper limit of $F_E(3.7 \text{ TeV}) < 2.91 \times 10^{-13} \text{ erg cm}^{-2} \text{ s}^{-1}$.

From *Chandra* measurements of thin X-ray filaments (Bamba et al. 2005), whose thickness is interpreted as the synchrotron cooling length of the radiating electrons, the actual field strength is $B \sim 300 \mu\text{G}$, following the arguments of BKV and Parizot et al. (2006). This field implies an IC gamma-ray energy flux of $f_\gamma(E_\gamma) < 1.4 \times 10^{-15} \text{ erg cm}^{-2} \text{ s}^{-1}$ which is two orders of magnitude below the measured upper limit.

4. Conclusions

Observations of Kepler's SNR with HESS result in an upper limit for the flux of VHE gamma rays from the SNR. In the context of an existing theoretical model (BKV) for the remnant, and assuming an ejected mass of $1.4 M_\odot$ and an explosion energy of 10^{51} erg in agreement with type Ia SN explosion models, the lack of a detectable gamma ray flux implies a distance of at least 6.4 kpc, which is the same as the upper limit derived by Reynoso & Goss (1999) from radio observations. Given that the gamma-ray flux effectively scales with E_{SN}^2 , a significantly higher explosion energy is excluded; a theoretically acceptable lower explosion energy of 0.8×10^{51} erg would lower the distance limit to 6 kpc.

Assuming a purely hadronic scenario, a standard type Ia SN explosion, and using 6.4 kpc as a lower limit for the distance, the HESS upper limit implies that the total energy in accelerated protons is less than 8.6×10^{49} erg.

In a synchrotron/IC scenario no strong constraints on the magnetic field can be obtained.

Acknowledgements. The support of the Namibian authorities and of the University of Namibia in facilitating the construction and operation of HESS is gratefully acknowledged, as is the support by the German Ministry for Education and Research (BMBF), the Max Planck Society, the French Ministry for Research, the CNRS-IN2P3 and the Astroparticle Interdisciplinary Programme of the CNRS, the UK Science and Technology Facilities Council (STFC), the IPNP of the Charles University, the Polish Ministry of Science and Higher Education, the South African Department of Science and Technology and National Research Foundation, and by the University of Namibia. We appreciate the excellent work of the technical support staff in Berlin, Durham, Hamburg, Heidelberg, Palaiseau, Paris, Saclay, and in Namibia in the construction and operation of the equipment.

References

- Aharonian, F. A., & Atoyan, A. M. 2000, *A&A*, 362, 937
- Aharonian, F. A., Atoyan, A. M., & Kifune, T. 1997, *MNRAS*, 291, 162
- Aharonian, F., Akhperjanian, A. G., Aye, K.-M., et al. (HESS Collaboration) 2004, *Astropart. Phys.*, 22, 109
- Aharonian, F. A., Akhperjanian, A. G., Aye, K.-M., et al. (HESS Collaboration) 2005, *A&A*, 430, 865
- Allen, G. E., Gotthelf, E. V., & Petre, R. 1999, *Proc. 26th ICRC*, Salt Lake City, 3, 480
- Baade, W. 1943, *ApJ*, 97, 119
- Badenes, C., Borkowski, K. J., & Bravo, E. 2005, *ApJ*, 624, 198

² $f(E) = E^2 F(E)$.

- Bamba, A., Yamazaki, R., Yoshida, T., Terasawa, T., & Koyama, K. 2005, *ApJ*, 621, 793
- Bandiera, R. 1987, *ApJ*, 319, 885
- Berezhko, E. G., & Ellison, D. C. 1999, *ApJ*, 526, 385
- Berezhko, E. G., Ksenofontov, L. T., & Völk, H. J. 2006, *A&A*, 452, 217
- Berge, D., Funk, S., & Hinton, J. 2007, *A&A*, 466, 1219
- Blair, W. P. 2005, 1604–2004: Supernovae as Cosmological Lighthouses, *ASP Conf. Ser.*, 342, 416
- Blair, W. P., Ghavamian, P., Long, K. S., et al. 2007, *ApJ*, 662, 998
- Cassam-Chenaï, G., Decourchelle, A., Ballet, J., et al. 2004, *A&A*, 414, 545
- Decourchelle, A., & Ballet, J. 1994, *A&A*, 287, 206
- Dickel, J. R., Sault, R., Arendt, R. G., Matsui, Y., & Korista, K. T. 1988, *ApJ*, 330, 254
- Doggett, J. B., & Branch, D. 1985, *AJ*, 90, 2303
- Drury, L. O., & Voelk, J. H. 1981, *ApJ*, 248, 344
- Drury, L. O., Aharonian, F. A., & Völk, H. J. 1994, *A&A*, 287, 959
- Feldman, G. J., & Cousins, R. D. 1998, *Phys. Rev. D*, 57, 3873
- Fich, M., Blitz, L., & Stark, A. A. 1989, *ApJ*, 342, 272
- Gaisser, T. K. 1990, *Cosmic rays and particle physics* (Cambridge and New York: Cambridge University Press)
- Hinton, J. A. 2004, *New Astron. Rev.*, 48, 331
- Hughes, J. P. 1999, *ApJ*, 527, 298
- Kinugasa, K., & Tsunemi, H. 1999, *PASJ*, 51, 239
- Lemoine-Goumard, M., Degrange, B., & Tluczykont, M. 2006, *Astropart. Phys.*, 25, 195
- Li, T.-P., & Ma, Y.-Q. 1983, *ApJ*, 272, 317
- Parizot, E., Marcowith, A., Ballet, J., & Gallant, Y. A. 2006, *A&A*, 453, 387
- Reynolds, S. P., Borkowski, K. J., Hwang, U., et al. 2007, *ApJ*, 668, L135
- Reynoso, E. M., & Goss, W. M. 1999, *AJ*, 118, 926
- Sankrit, R., Blair, W. P., Delaney, T., et al. 2005, *Adv. Space Res.*, 35, 1027
- Smith, A., Peacock, A., Arnaud, M., et al. 1989, *ApJ*, 347, 925
- Vink, J. 2008, *ApJ*, submitted [arXiv:0803.4011]
- ⁷ IRFU/DSM/CEA, CE Saclay, Gif-sur-Yvette, France
- ⁸ University of Durham, Department of Physics, UK
- ⁹ Unit for Space Physics, North-West University, Potchefstroom, South Africa
- ¹⁰ Laboratoire Leprince-Ringuet, École Polytechnique, CNRS/IN2P3, Palaiseau, France
- ¹¹ Laboratoire d'Annecy-le-Vieux de Physique des Particules, CNRS/IN2P3, Annecy-le-Vieux, France
- ¹² Astroparticule et Cosmologie (APC), CNRS, Université Paris 7 Denis Diderot, 10, Paris, France UMR 7164 (CNRS, Université Paris VII, CEA, Observatoire de Paris)
- ¹³ Dublin Institute for Advanced Studies, Dublin, Ireland
- ¹⁴ Landessternwarte, Universität Heidelberg, Königstuhl, Heidelberg, Germany
- ¹⁵ Laboratoire de Physique Théorique et Astroparticules, CNRS/IN2P3, Université Montpellier II, France
- ¹⁶ Universität Erlangen-Nürnberg, Physikalisches Institut, Erlangen, Germany
- ¹⁷ Laboratoire d'Astrophysique de Grenoble, INSU/CNRS, Université Joseph Fourier, France
- ¹⁸ Institut für Astronomie und Astrophysik, Universität Tübingen, Germany
- ¹⁹ LPNHE, Université Pierre et Marie Curie Paris 6, Université Denis Diderot Paris 7, CNRS/IN2P3, Paris, France
- ²⁰ Institute of Particle and Nuclear Physics, Charles University, Prague, Czech Republic
- ²¹ Institut für Theoretische Physik, Lehrstuhl IV: Weltraum und Astrophysik, Ruhr-Universität Bochum, Germany
- ²² University of Namibia, Windhoek, Namibia
- ²³ Obserwatorium Astronomiczne, Uniwersytet Jagielloński, Kraków, Poland
- ²⁴ Nicolaus Copernicus Astronomical Center, Warsaw, Poland
- ²⁵ School of Physics & Astronomy, University of Leeds, UK
- ²⁶ School of Chemistry & Physics, University of Adelaide, Australia
- ²⁷ Toruń Centre for Astronomy, Nicolaus Copernicus University, Toruń, Poland
- ²⁸ European Associated Laboratory for Gamma-Ray Astronomy, jointly supported by CNRS and MPG
-
- ¹ Max-Planck-Institut für Kernphysik, Heidelberg, Germany
e-mail: dominik.hauser@mpi-hd.mpg.de
- ² Yerevan Physics Institute, Armenia
- ³ Centre d'Étude Spatiale des Rayonnements, CNRS/UPS, Toulouse, France
- ⁴ Universität Hamburg, Institut für Experimentalphysik, Germany
- ⁵ Institut für Physik, Humboldt-Universität zu Berlin, Germany
- ⁶ LUTH, Observatoire de Paris, CNRS, Université Paris Diderot, Meudon, France